GEOPHYSICAL RESEARCH LETTERS, VOL. 24, NO. 23, PAGES 3053-3056, DECEMBER 1, 1997

S–wave structure of the American Southwest and Mexico from single–station broadband data

Laura E. Jones, Hanneke Paulssen and Everhard Muyzert

Department of Geophysics, University of Utrecht, Postbus 80.021, 3508 TA Utrecht, The Netherlands

Abstract. We investigate *S* velocity structure beneath the Southwestern U.S. and Mexico using upper mantle turning *S* waves and surface waves. The data are tangential component records from Baja California, Mexican and Central American events recorded at broadband station ANMO (Albuquerque, New Mexico). Study geometry allows investigation of the variation of *S* structure with source-receiver azimuth for sources from Baja to Yucatan. The narrow backazimuthal sector studied comprises a transition from oceanic to tectonic to more 'continent-like' structure. We document this transition in the lithosphere and upper mantle to roughly 450 km depth.

Introduction

While the Southwestern United States area is well studied, adjacent Mexico has attracted much less attention, due in part to lack of the station coverage necessary for regional waveform studies. Recent surface wave studies exist [cf. Alsina et al., 1996; van der Lee and Nolet, 1997b], but are mutually inconsistent in this region.

In the present study, we obtain a family of *S* velocity models for lithospheric and uppermost mantle structure in Mexico and Southwestern U. S. from body and surface wave data. Earthquakes along the Mexican coast from Baja to Yucatàn, recorded at station ANMO (Albuquerque, New Mexico) form a natural profile of records ranging from 14° to 30° epicentral distance [Figure 1]. The narrow backazimuthal sector covered by these paths encompasses a transition from oceanic to tectonic to more 'continent-like' structure.

The Observations

80 events ($M \geq 5$) at epicentral distances between 14° and 30°, depths between 20 and 70 km, and backazimuths between 130° to 160° were selected [Figure 1]. These events provide clean *S* waves which turn beneath Mexico and the Southwestern United States, and *Love* waves which should sense the effects of a lithospheric and crustal transition between oceanic, tectonic and continental structures. Prior to analysis, seismograms were integrated to displacement, rotated, and travel-time corrected for a uniform source depth of 25 km. For the body wave study, a Butterworth bandpass filter with corners at 0.005 and 5 Hz was applied in two passes to the transverse components. For the surface wave study, a subset of high-quality events was selected, and a number of relevant bandpasses applied (see below).

Paper number 97GL02890.
0094-8534/97/97GL-02890$05.00

Body Wave Modeling

Initial body wave modeling was done using three reference models, each chosen to represent the possible range of structure present [Figure 2]. Travel time curves were computed for the three models using a WKBJ routine [Chapman, 1978], and these curves were plotted in reduced time on top of the entire data profile. To represent youthful, tectonically active structure, we chose model WUS, a model for Western U. S. structure, derived from higher mode Rayleigh waves and featuring a pronounced low velocity zone [Cara, 1979]; and model TNA, a regional model for tectonic North American structure obtained from *S* and *SS* modeling [Grand and Helmberger, 1984]. To represent stable structure, we selected PEM-C, a model for continental structure, featuring a thick fast lid [Dziewonski et al., 1975]. The structures are different above the transition zone (440 km); below they are nearly identical.

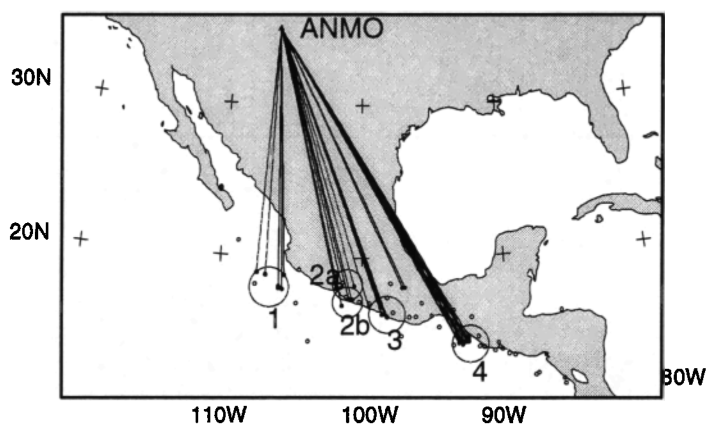

Figure 1. Map of study area with location of station ANMO (Albuquerque, New Mexico). Open symbols indicate events used in body-wave modeling, while filled indicate earthquakes used in both Partitioned Waveform Inversion (PWI) [Nolet, 1990] and body wave studies. Earthquake clusters used in the PWI study are numbered and circled.

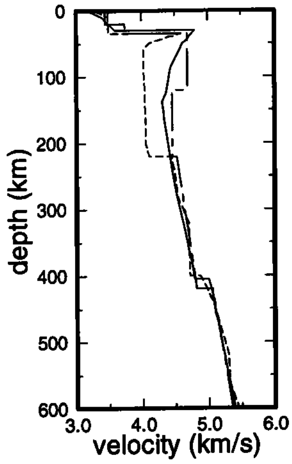

Figure 2. Reference models used in preliminary study. TNA′ (Grand and Helmberger, 1984) is shown in solid line, WUS (Cara, 1979) in short dash and PEM-C (Dziewonski et al., 1975) in long dash.

A low velocity zone is required to explain the absence of early S arrivals turning above the transition zone in the epicentral distance range of 14° to 19°. Model WUS explained the late S arrivals in this epicentral distance range, but was on average too slow [Figure 3, in yellow]. The other extreme, represented by Model PEM-C, is up to 10 seconds fast for distances of 18° to 22°, as well as producing unwanted first S arrivals from 14° to 19° [Figure 3, in blue]. Model TNA appears relatively accurate from 19° to 22°, but produces undesirable S arrivals in the shadow zone from 14° to 17°, and is too slow at distances greater than 23°. Thus at distances of 14° to 19°, 19° to 22°, and 22° to 25°, respectively, different lithospheric and uppermost mantle structures are required. Model TNA lies between the extremes represented by WUS and PEM-C, and thus forms an acceptable average starting model for the region of interest. TNA′ [Figure 3, in red] was obtained by adjusting TNA by trial and error to fit our data profile: lid velocities were increased by 5%, and the velocities within the LVZ decreased slightly. However, from body wave modeling it was clear that no single one-dimensional model would fit the entire profile.

Surface Wave Modeling

Further one-dimensional modeling via a partitioned waveform inversion of fundamental and higher mode Love waves was motivated by the lateral heterogeneity evident in the body wave profiles and from preliminary modeling. In the method employed, the observed wavefield is broken up into component phases (and their relevant frequencies) and each wavegroup is inverted simultaneously. Synthetics for the inversion are computed by summation of normal modes.

The inversion scheme is based on a nonlinear waveform-fitting procedure similar to (PWI), and is as follows: using a conjugate gradient scheme, we minimize a misfit function

$$M = \sum_{i=1}^{N} \int [D_i(t) - S_i(t)]^2 dt + \gamma_m$$

where $D(t)$ are filtered observations, $S(t)$ appropriate synthetics, γ_m is smoothness of the velocity model, computed using a two-point smoothing operator, and M is summed over N events contributing waveforms to the inversion. Data and synthetics are given phase velocity windows appropriate to the phase of interest. In the process of inversion, we model the entire wavetrain from S to the fundamental mode in three frequency bands (two fundamental mode windows between 0.005 – 0.01 Hz and 0.01 – 0.025 Hz, and one higher mode window around the S and SS phases at frequencies of 0.0125 – 0.10 Hz). At the distances considered here, the S and SS phases cannot be separated, so a window containing both is used. To prevent the inversion from falling into local minima, the fundamental modes are inverted initially and depth resolution increased by iteratively adding higher modes and higher frequencies to the inversion.

Clusters of events within one degree (backazimuth and distance) of each other were selected from the original profile for a series of PWI grouped by epicentral distance and backazimuth. These clusters range in epicentral distance from 16° to roughly 23°, ranging eastward from near the tip of Baja to just southeast of the Yucatan [Figure 1]. Each group comprises waveforms from 4 to 13 events of varying depths. We include deeper events in each cluster, where available, to

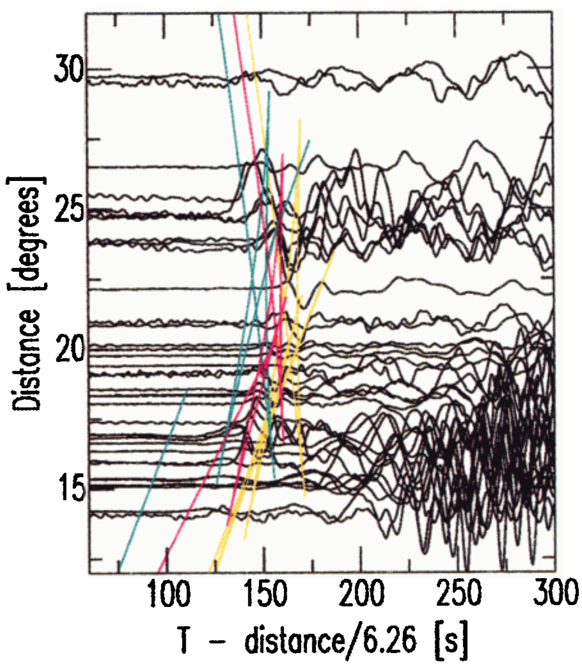

Figure 3. Travel time curves for each of the reference models, shown superimposed on the dataset. PEM-C is shown in aqua, WUS in yellow, and TNA′ in red.

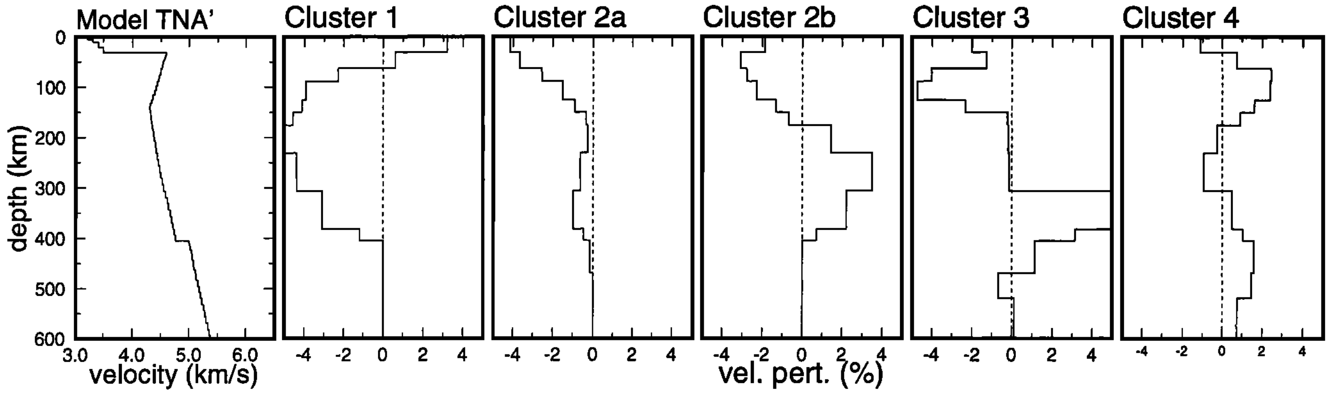

Figure 4. Final models obtained in the PWI study. Reference model TNA′ is shown in the leftmost panel, and velocity perturbations to TNA′ for each cluster are shown in the successive panels.

improve depth resolution in the inversions. Source locations and CMT moment tensor solutions were taken from the ISC catalogs for events prior to September 1993, or the NEIC Preliminary Determination of Epicenters for more recent earthquakes. The accuracy of these sources was tested initially by preliminary waveform modeling using whole waveforms; events with visibly inaccurate sources or depths were discarded.

Models TNA′ and PEM-C [Figure 2] were used as initial models for the inversions. We discuss models for each of four azimuthal clusters [Figure 4], west to east, respectively, below. Waveform fits for the final models were generally very good [Figure 5]. We show results from model TNA′; using PEM-C as initial model yields similar results. Resolution of the inversions was tested by tradeoff analysis between damping (γ_m) and data misfit, and further by checkerboard synthetic tests. γ_m was selected by trial and error to minimize misfit and maximize variance reduction. Resolution tests showed, on average, good resolution for all clusters down to depths of 400 to 450 km. Resolution was improved for larger clusters with better depth distribution. Below 450 km depth, resolution is poor.

Cluster 1: Oceanic Structure This group included 6 events at epicentral distances of roughly 16°, located south of the tip of Baja California [Figures 1 and 4]. Preliminary modeling suggests that the initial model TNA′ is too fast both for longer period energy traveling in the crust and lithosphere, and for diving higher mode (*S* and *SS*) phases. Inversions using Love waves from this cluster resulted in structure typical of oceanic crust and upper mantle. Crustal velocities were increased by roughly 3% over model TNA′, while values from 50 km to roughly 200 km were decreased by up to 4% [Figure 4]. Average variance reduction for this cluster was 48%.

Clusters 2 and 3: Transitional Structure Inversions for these clusters revealed evidence of structural complexity on wavelengths of less than 100 km, and clearly suggested a transitional zone between the oceanic-like structure beneath the group 1 sector and the more continent-like average structure beneath the group 4 sector (below). Average variance reductions for groups 2a, 2b and 3 were 61%, 49% and 52%, respectively.

The events in cluster 2, at roughly 17° to 18° epicentral distance, were further divided into groups 2a and 2b, based on location [Figure 1]. Those in group 2a (17°) lie north of group 2b events, though the backazimuthal sector of both groups is roughly identical. Inversions of the fundamental mode waveforms for both groups yield crustal and lid velocities reduced by up to 4% (relative to reference model TNA′) down to depths of 100 km. However, the body waves and higher modes yield slightly *reduced* (1% relative to TNA′) upper mantle velocities at depths of roughly 200 to 400 km for group 2a events and velocities *increased* by up to 3% at similar depths for the group 2b events located around one degree south. This may be explained by mode coupling due to a small-scale low velocity feature (i.e., the Mexican Volcanic belt) present in the path. In this

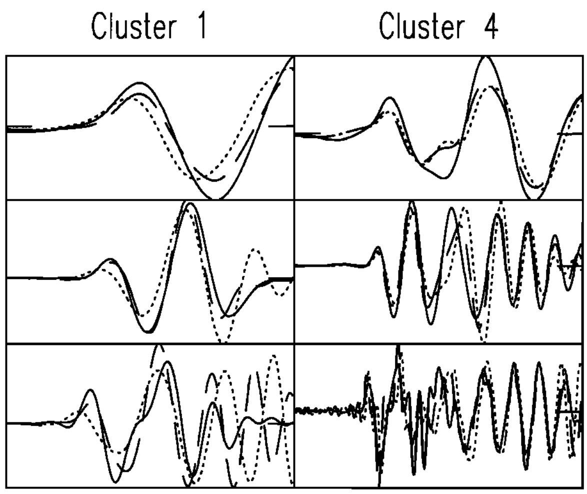

Figure 5. Example waveform fits for initial (short dash) and final (long dash) models, plotted against data (solid line) for events in Groups 1 and 4. Average variance reductions are 36% and 47%, respectively. Waveform fits are shown in three bandpasses: 0.005 - 0.01 Hz, 0.01 - 0.025 Hz, and 0.0125 - 0.10 Hz.

scenario, only fundamental modes, from which crustal and lithospheric velocities are determined, are sensing this feature, while body waves (i.e., higher modes) dive below. This would result in a lithospheric and crustal structure which is anomalously slow; a result largely correlatable to event location with respect to the localized low velocity feature. Alternatively, body waves from events in group 2b, which lie south of those in group 2a and along the coast, may be passing through a localized *high* velocity body, such as the Cocos plate subducting along the Southwest and Southeast Mexico subduction zones. Thus in either case, the model required to satisfy both the body waves and surface waves would be at least two dimensional.

However, cluster 3 events, at epicentral distances of 19^o to 20^o, give inversion results arguably consistent with those of group 2b. The reference model was fast for all frequency bands, though less markedly so for the higher modes. The inversions were repeated for two clusters of (co-located) events; results for both sets of inversions were similar. Upper mantle structure was reduced by nearly 5% to depths of about 120 km, and a high-velocity feature (increases of over 5% relative to TNA$'$) appears at depths of about 300 to 450 km. The high velocity feature is robust: it is resolved by every set of inversions, though some parameterizations result in a more diffuse feature.

Cluster 4: Continent-like Structure Inversions using data from a large, spatially tight swarm of 12 small earthquakes in 1993 revealed structure more typical of continents. Inversions for both reference models reveal similar structure: increased lithospheric velocities (up to 3%) down to 150 km, the suggestion of a low velocity zone in the uppermost mantle from 180 to 300 km depth, and again, an increase (2%) in velocity from just above to just below the transition zone. Note that the high velocity feature appears at progressively lower depths from west to east across clusters 2B to 4. Average variance reduction for this cluster of 16 events was 36%.

Discussion

Prior studies in several regions have yielded evidence for substantial small–scale upper mantle heterogeneity. Paulssen [1987] found evidence from body waves of small–scale heterogeneity of as much as 4% (S–waves) down to depths of 400 km across Europe. Work by Alsina et al. [1996] revealed both large-scale west to east velocity variation across the United States and Mexico as well as smaller scale heterogeneity. Their study generally agrees with work by Grand [1987, 1994], except in the Yucatan region, where the former authors observe relatively high velocities. In this study we also find evidence for west to east velocity variation in the form of a transition from oceanic to 'continent–like' structure, with low upper mantle velocities (west) grading into higher upper mantle velocities and a thicker lid (east, in the Middle America Trench area south of Yucatan). Group 1 source–receiver paths travel through a broad low–velocity region running from Baja California to Western Mexico to the Basin and Range, also imaged by Alsina et al. [1996], and consistent with a western US 'slab window' imaged by van der Lee and Nolet [1997a,b]. However, further east (groups 2a through 3), we find relatively slow lithosphere and uppermost mantle, due perhaps to the presence of the Mexican Volcanic belt lying just north of the source area. Furthermore, from west to east (clusters 2a through 3) we resolve a descending high–velocity feature at depths ranging from 200 (west, group 2a) to 500 km (east, group 4), the presence of which is supported by good waveform fits for all three event clusters. A similar feature, interpreted as subducted trailing fragments of the Farallon plate, has also been imaged by van der Lee and Nolet [1996a,b], using a much larger data set. The appearance of this high–velocity feature in our study is either due to the mode coupling from a localized shallow low velocity feature such as the Mexican Volcanic belt, or may indeed be an expression of deeper structure, such as the presently subducting Cocos plate, or remnants of the fossil Farallon plate.

Acknowledgments. Data were provided by the IRIS Data Management Center. Geodynamics Research University (Utrecht University) contribution number 97.009.

References

Alsina, D., R. L. Woodward and R. K. Snieder, Shear wave velocity structure of North America from large–scale waveform inversions of surface waves, *J. Geophys. Res.*, 101, 15969–15986, 1996.

Chapman, C. H., A new method for computing synthetic seismograms, *Geophys. J. R. Astr. Soc.*, 54, 481-518, 1978.

Cara, M., Lateral Variations of *S* velocity in the upper mantle from higher Rayleigh modes, *Geophys. J. R. astr. Soc.*, 57, 649–670, 1979.

Dziewonski, A.M., A. L. Hales, and E. R. Lapwood, Parametrically simple Earth models consistent with geophysical data, *Phys. of Earth and Planet Int.*, Vol. 10, pp. 12–48, 1975.

Grand, S. Tomographic inversion for shear velocity beneath the North American Plate, *J. Geophys. Res.*, *92*, 14,065–14,090, 1987.

Grand, S. and D. V. Helmberger, Upper mantle shear structure of North America, *Geophys. J. R. Astron. Soc.*,*76*, 399-438, 1984.

Grand, S. P., Mantle shear structure beneath the Americas and surrounding oceans, *J. Geophys. Res.*,99, 11591-11621, 1994.

Nolet, G., Partitioned waveform inversion and two-dimensional structure under the Network of Autonomously Recording Seismographs (NARS), *J. Geophys. Res.*, *95*, 8499–8512, 1990.

Paulssen, H., Lateral heterogeneity of Europe's upper mantle as inferred from modelling of broad–band body waves, *Geophys. J. R. Astr. Soc.*, 91, 171–199, 1987.

van der Lee, S. and G. Nolet, The upper-mantle S-velocity structure of North America, in press, *J. Geophys. Res.*, 1997.

van der Lee, S. and G. Nolet, Seismic image of the subducted trailing fragments of the Farallon plate, *Nature*, 386, 266-269, 1997.

University of Utrecht, Postbus 80.021, 3508 TA Utrecht, The Netherlands

(received June 12, 1996; revised May 27, 1997;
accepted September 10, 1997.)